Available online at www.sciencedirect.com
ScienceDirect
Carbon 45 (2007) 2253–2259
CARBON
www.elsevier.com/locate/carbon

Synthesis of nitrogen-doped horn-shaped carbon nanotubes by reduction of pentachloropyridine with metallic sodium

Xingcai Wu *, Yourong Tao, Changjie Mao, Lele Wen, Junjie Zhu

Key Laboratory of Mesoscopic Chemistry of MOE, The State Key Laboratory of Coordination Chemistry, School of Chemistry and Chemical Engineering, Nanjing University, Nanjing 210093, PR China

Received 23 November 2006; accepted 18 June 2007
Available online 28 June 2007

Abstract

Nitrogen-doped horn-shaped carbon nanotubes (CNTs) have successfully been prepared by reducing pentachloropyridine with metallic sodium at 350 °C. A typical CNT has an open-end diameter of ~2 μm, a close-end diameter of ~0.3 μm, a wall thickness of ~30 nm, and a length up to 8 μm. TEM observation indicates that the CNTs account for ~30% of the products, and the rest is solid and hollow carbon nanospheres (CNSs) with a diameter of about 50–290 nm. Elemental analysis shows that the N/C atomic ratio of the carbon nanostructures is about 0.0208. XRD and HRTEM measurements reveal that the CNTs are amorphous. To understand the growth process and refine the growth condition, various control experiments have been finished. At last, a sodium-catalysis-reduction solid–liquid–solid growth mechanism of the CNTs has been suggested on the basis of the experiments.

1. Introduction

Since the discovery of carbon nanotubes (CNTs) [1], considerable attention has been attracted for synthesizing them due to their unique properties [2] and potential applications [3–5]. Recent research has shown that some physical properties of the CNTs usually depend on their structures, whereas practical applications demand special morphologies, so a great effort has been made to control the structure and morphology of the CNTs by different synthetic methods. People have so far synthesized various structural and morphological CNTs such as multi-, single-, and double-walled [6,7], as well as Y-, bamboo-, and cone-shaped CNTs [8,9]. In addition, the research has still shown that the incorporated N in carbon nanostructures can enhance their mechanical, energy storage, and electric properties [10]. Hence the preparation of the N-doped CNTs has been concerned widely, and many methods including magnetron sputtering [11], arc discharge [12], chemical vapor deposition [13], and chemical reaction of small molecule carbon halides with NaN_3 [14] have been employed for this purpose. Jiang et al. once prepared hollow and bamboo-shaped CNTs using reduction of hexachlorobenzene (C_6Cl_6) by metallic potassium in the presence of Co/Ni catalyzer and in benzene solution, and thought that the CNTs formed from assembly of carbon six-number-ring [15]. Can we prepare a C_5N-type nanotube by reduction of pentachloropyridine (C_5NCl_5) with metallic sodium according to the thought? To reduce effect of various factors on the reaction, benzene and Co/Ni catalyser were not used in our experiment. Finally, we obtained the horn-shaped CNTs, but the N/C ratio is much lower than that (0.2) of C_5N-type nanotubes. To our knowledge, the N-doped horn-shaped CNTs have not been reported so far.

2. Experimental

2.1. Sample preparation

Two grams of pentachloropyridine and 1.5 g metallic sodium were placed into stainless steel autoclave with 25 mL capacity, and then the autoclave was sealed, heated to 350 °C, and maintained at the temperature

* Corresponding author. Fax: +86 25 83317761.
E-mail address: wuxingca@nju.edu.cn (X. Wu).

0008-6223/$ - see front matter © 2007 Elsevier Ltd. All rights reserved.
doi:10.1016/j.carbon.2007.06.024

for 10 h, and then cooled to room temperature in the furnace naturally. The dark products were collected and washed sequentially with absolute ethanol, concentrated salt acid aqueous solution, and distilled water to remove residual impurities. The final products were dried at 100 °C in air for 4 h, yielding about 0.40 g of the products. The same experiments were finished at 150, 250, 300 and 400 °C, respectively.

2.2. Measurements and characterization

X-ray diffraction (XRD) patterns of the products were recorded on Philips X' pert X-ray diffractometer with graphite monochromatized Cu Kα-radiation. The morphology of the products was observed on a LEO-1530 VP field emission scanning electron microscope (SEM) with the selected area energy-dispersive X-ray spectrometry (EDX). Transmission electron microscope images were recorded on a JEOL-JEM 200CX transmission electron microscope (TEM), using an accelerating voltage of 200 kV. The microstructures of the carbon nanotubes were characterized by a JEOL Model JEM-2100 high-resolution transmission electron microscope with a point resolution of 0.19 nm (HRTEM). Micro-Raman spectra were recorded at ambient temperature on a T64000 Raman spectrometer at room temperature. All Raman lines obtained were treated with a linear baseline subtraction. C and N elements were quantified by a Foss Heraeus CHN-O-Rapid elemental analyzer (Ger.). In addition, the C–N bond was confirmed by X-ray photoelectron spectroscopy (XPS, VG ESCALAB MKII) excited by an X-ray source of Mg Kα ($h\nu < 1253.6$ eV) in an ultrahigh vacuum chamber with a base pressure of $<2 \times 10^{-8}$ Torr.

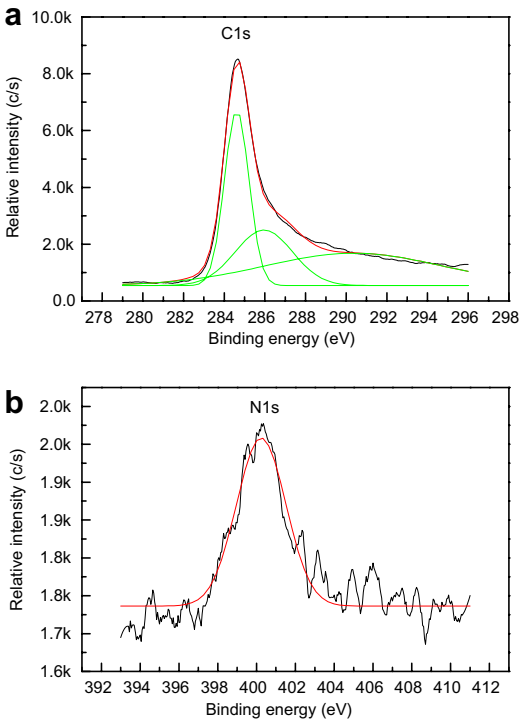

Fig. 2. XPS spectra of the sample prepared at 350 °C. (a) C1s; (b) N1s.

3. Results and discussion

3.1. Microstructure and morphology of the products

Fig. 1a–c are the SEM images of the sample prepared at 350 °C, which show horn-shaped CNTs. Generally, one end of the CNT is open while another is close, and open-end diameter is greater than close-end one (confirmed by TEM observation shown in Fig. 3c). Fig. 1a reveals that a CNT (as white arrow indicates) has an open-end diameter of about 0.8 μm, a close-end diameter of about 0.3 μm,

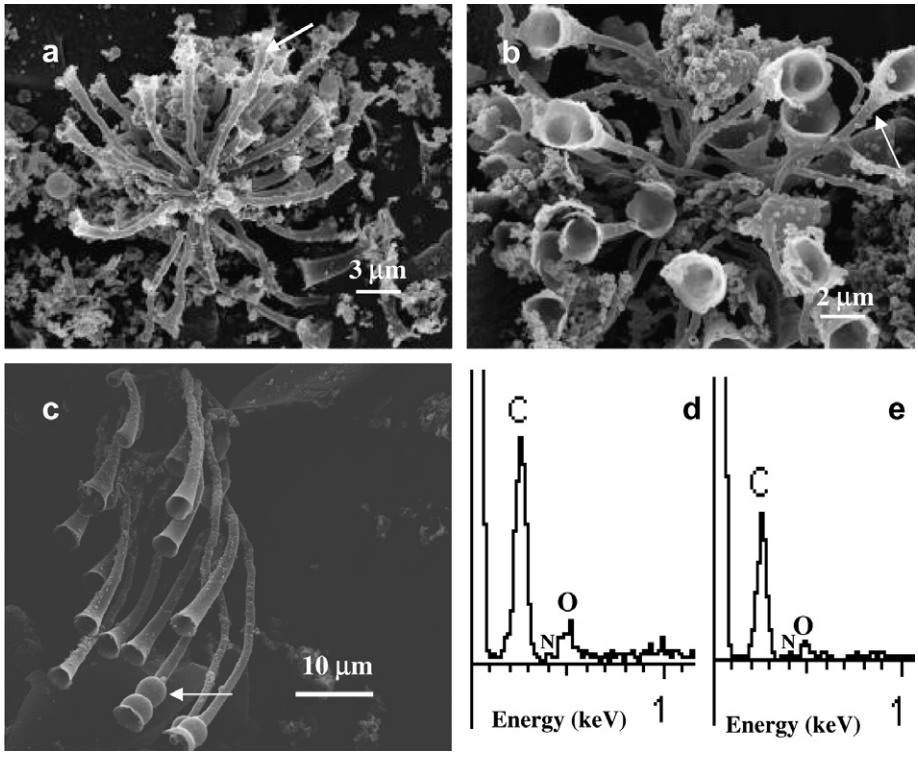

Fig. 1. (a–c) SEM images of the horn-shaped CNTs prepared at 350 °C; (d) EDX spectrum of a single horn-shaped CNT; (e) EDX spectrum of carbon particle.

and a length up to 8 μm. Fig. 1b shows that a CNT (as white arrow indicates) has an open-end diameter of about 2 μm, a close-end diameter of about 0.3 μm, and a length up to 7 μm. A horn-like CNT with dumbbell-shaped open-end has been discovered as white arrow indicates in Fig. 1c. Typical EDX spectra of a single CNT and carbon particle (CP) are shown in Fig. 1d and e, respectively, and both have extremely weak peaks at nitrogen position. It confirms that nitrogen exists in CNTs and CPs. Because nitrogen content is extremely small, it is difficult to quantify nitrogen content by EDX. Considering that the CNTs and the CPs are formed under same condition, their nitrogen content should be approximate, so an average N/C atomic ratio is quantified by elemental analyzer. Fig. 2a and b display the C1s and N1s spectra of the sample prepared at 350 °C, respectively. The peaks of C1s spectrum at 284.6 and 286.0 eV through Gaussian fitting are assigned to C1s in graphite and the adsorbed CO_2 on the powders' surface, respectively, whereas the weak peak at 290.4 eV is attributed to the π–π^* transitions accompanying the C1s excitation [16]. The peak at 400.3 eV through Gaussian fitting comes from the pyridine-like N atoms, i.e. the nitrogen in a ring structure folding only two carbon atoms [17]. The N/C atomic ratio is quantified as 0.0253 by XPS measurement.

TEM images (Fig. 3a–c) further confirm that the CNTs are of horn-shaped morphology. The CNTs account for ~30% of the products through observation of TEM and SEM, and the rest consists of solid and hollow carbon nanospheres (CNSs) with a diameter of about 50–290 nm, shown in Fig. 3d. HRTEM image (Fig. 3e) reveals that the wall thickness of the CNT is about 30 nm, whereas fringe images (insets in Fig. 3e and f) confirm that the nanostructures are amorphous.

For knowing the growth condition of the CNTs, the same experiments at various temperatures such as 150, 250, 300, and 400 °C have been carried out, respectively. The results shows that CNTs can not form below 300 °C (Fig. 4a–c). However, when synthesis temperature reaches 400 °C, the tube ratio decreases, only accounting for about 15% of the products (Fig. 4d). The N/C atomic ratios of the products prepared at different reaction temperatures are quantified by elemental analyzer, and included in Table 1. With synthesis temperatures increasing, the nitrogen content decreases, and are obviously lower than that (0.20) of

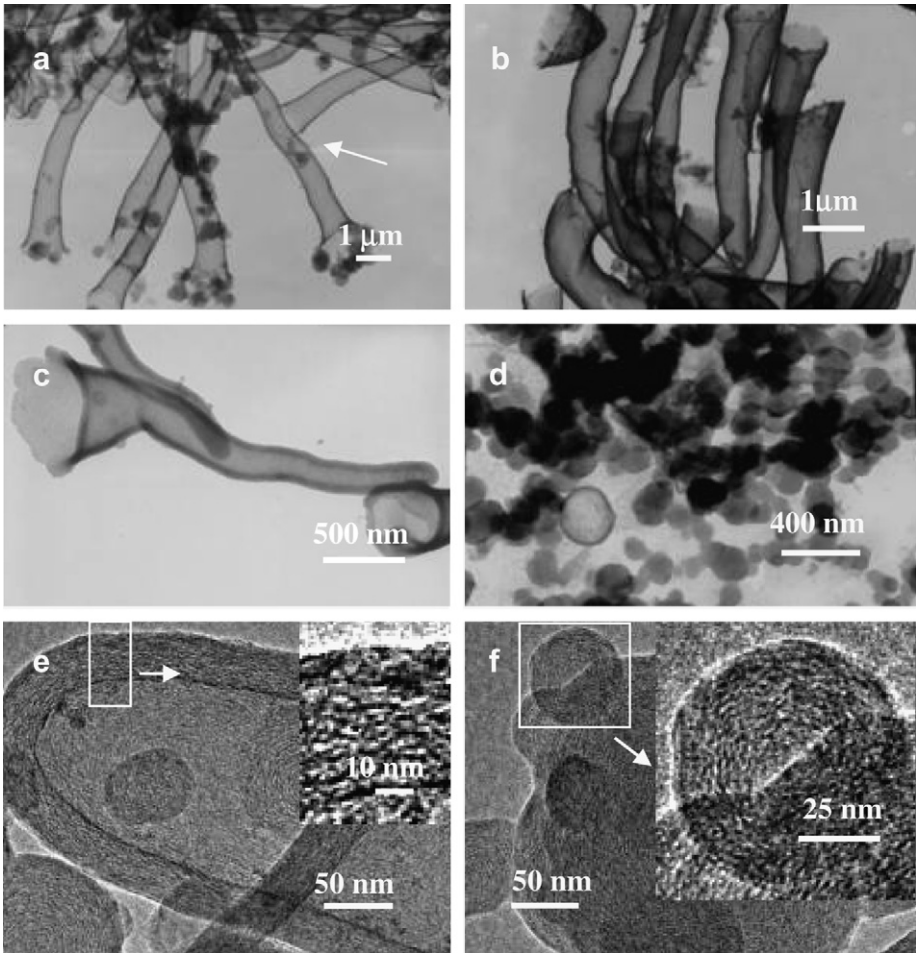

Fig. 3. Microstructure of the products prepared at 350 °C. (a, b) TEM images of the horn-shaped CNTs; (c) TEM image of a single horn-shaped CNT; (d) TEM image of carbon nanospheres; (e) HRTEM image of a single horn-shaped CNT; (f) HRTEM image of solid CNSs. Insets in (e) and (f) are magnified images in box, respectively.

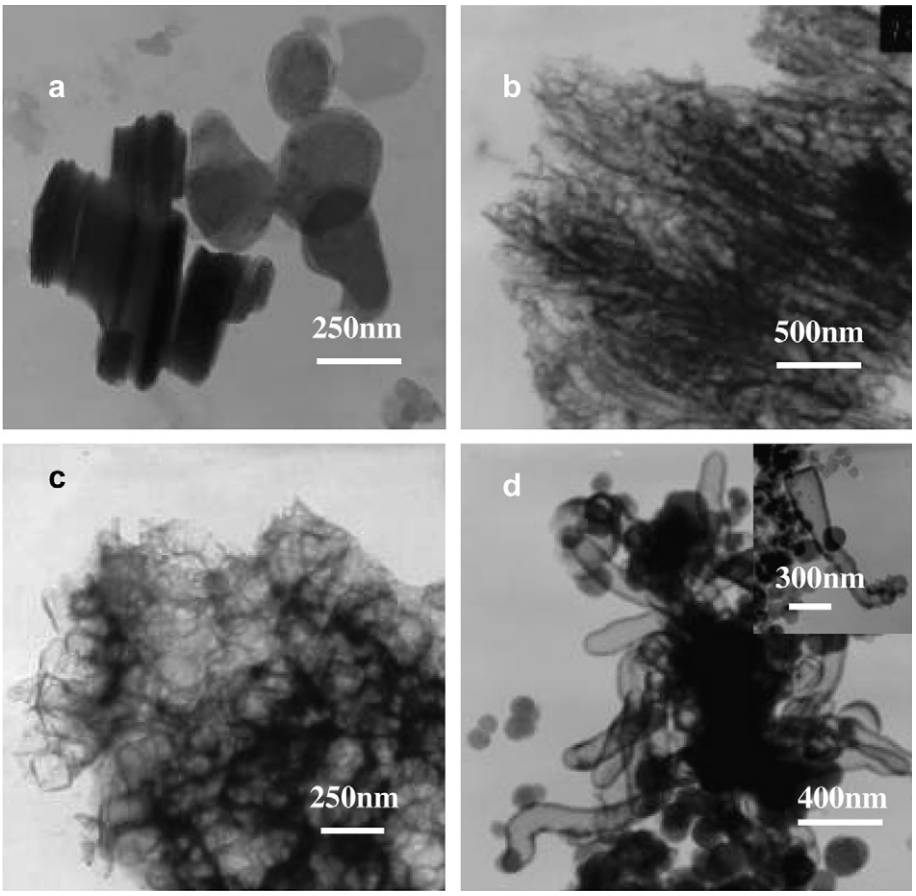

Fig. 4. TEM images of the carbon nanostructures prepared at various temperature. (a) 150 °C; (b) 250 °C; (c) 300 °C; (d) 400 °C.

Table 1
Relativity of Raman shifts, I_D/I_G, and N/C atomic ratios of the samples to reaction temperatures

Numbers of samples	Reaction temperatures (°C)	N/C atomic ratios	D-bands (cm^{-1})	G-bands (cm^{-1})	I_D/I_G
1	150	0.127	1364.2	1589.3	1.93
2	250	0.120	1361.4	1588.4	2.74
3	300	0.108	1357.9	1587.3	2.13
4	350	0.0208	1361.3	1589.9	2.38
5	400	0.0207	1360.0	1590.2	1.82

C_5N-type nanostructures, which suggests that pyridine rings broke during the formation of the CNTs.

In addition, XRD patterns still indicate the products obtained at 150–350 °C are amorphous (Fig. 5a–c). As is shown in Fig. 5d, XRD pattern of the products obtained at 400 °C can be indexed as hexagonal graphite structure (JCPDS No. 75-1621), and calculated d value of (002) plane from Bragg equation is 0.341 nm, approaching graphite interlayer spacing of the reported CNTs [18]. It shows that the crystallinity of the products at 400 °C is improved obviously. When the products were washed with concentrated salt acid for several times, even if treated with a mixture of concentrated salt acid and nitric acid, the impure XRD peak ($d = 0.2805$ nm) of the products could not yet be removed. Hence we think that the impure peak could originate from another typical carbon (JCPDS No. 46-0943).

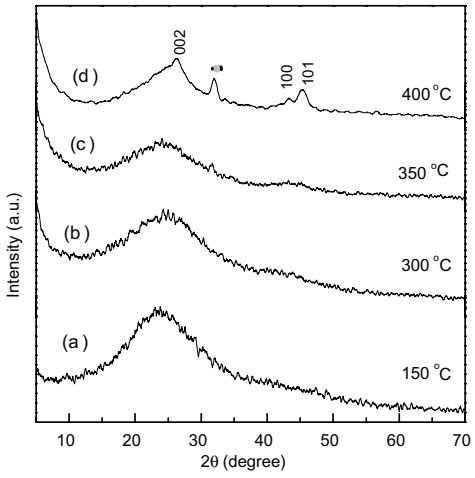

Fig. 5. XRD patterns of the products prepared at various temperature. (a) 150 °C; (b) 300 °C; (c) 350 °C; (d) 400 °C.

3.2. Raman spectroscopy

Fig. 6(a–e) shows the Raman spectra of the samples prepared at different temperature, which are of similar pat-

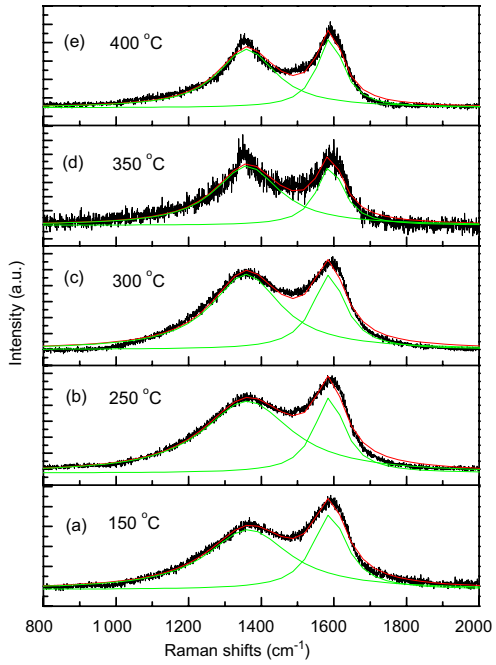

Fig. 6. Raman spectra of the samples prepared at various temperature. (a) 150 °C; (b) 250 °C; (c) 300 °C; (d) 350 °C; (e) 400 °C.

terns, and the Raman shifts at ~1360 and ~1600 cm^{-1} correspond to the graphite's D- and G-band, respectively. The D-band is disorder-induced and associated with optical phonons close to the K point of the Brillouin zone in graphite and carbon nanotubes, whereas the G-band is usually regarded as a Raman-allowed Γ point vibration corresponding to the optical phonon mode of E_{2g} symmetry (in-plane stretching vibration mode) in graphite and often called tangential mode for carbon nanotubes [19]. For comparison, all the Raman spectra were fitted with Lorentzian function curve, and the results were also included in Table 1. For example, the Raman shifts of the sample prepared at 350 °C are 1361.3 (D-band) and 1589.9 cm^{-1} (G-band), respectively, while the I_D/I_G ratio is ~2.38 (Fig. 6d). The Raman shifts of the sample prepared at 400 °C are 1360 (D-band) and 1590.2 cm^{-1} (G-band), respectively, whereas the I_D/I_G ratio is 1.82, which indicates the improvement of the products' crystallinity, however, the I_D/I_G ratios of all samples are higher than the I_D/I_G ratio (=0.85–1.3) of the recent-report CNTs by CVD thermal decomposition of acetylene, etc. [20], which indicate greater lattice distortions in the curved graphene sheets or disorder in sp^2-hybridized carbon. It is attributable that nitrogen incorporated into graphene plane causes distortion of graphene plane. Certainly, low reaction temperature can also lead to low crystallinity of CNTs. On the basis of Raman data, there is a tendency that D-band upshifts while G-band downshifts with the increase in the N/C ratios, which is almost agreeable to the reported results [21].

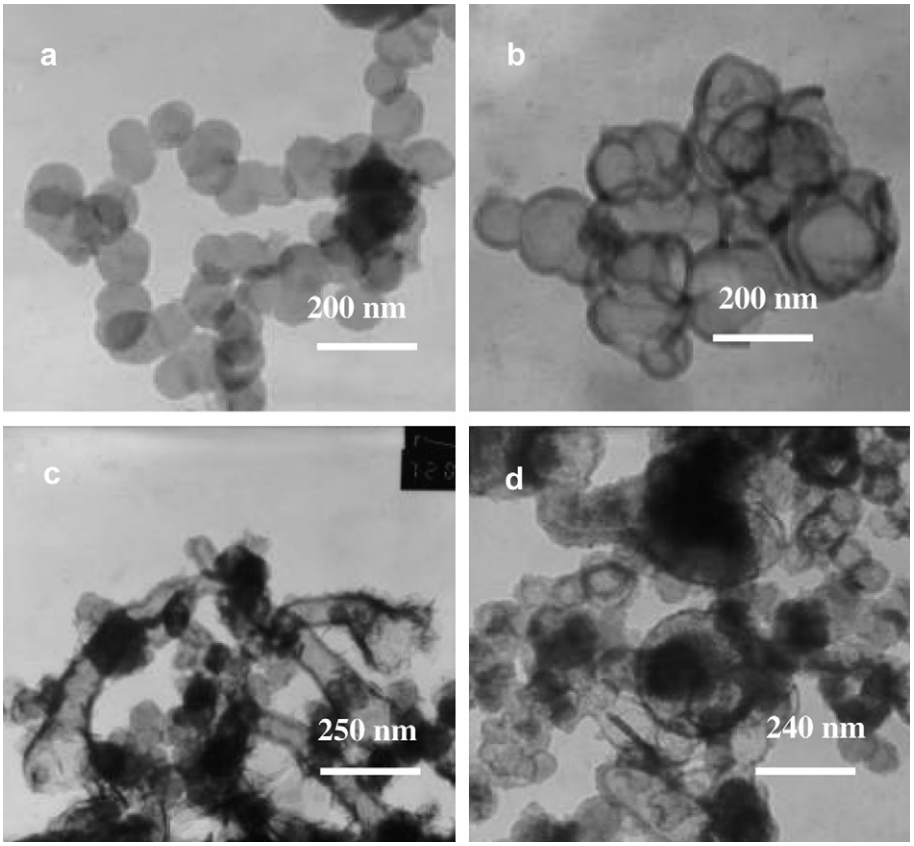

Fig. 7. TEM images of the samples prepared in different reaction temperatures at 350 °C. (a, b) 3 h; (c, d) 6 h.

3.3. Growth mechanism

The same experiments were done in different reaction time at 350 °C in order to understand the growth process. When the reaction took 3 h, the products were only hollow and solid CNSs (Fig. 7a and b), and the hollow CNSs accounted for about 20%. When the reaction took 6 h at 350 °C, the products were the mixture of short horn-shaped CNTs (Fig. 7c) and hollow and solid CNSs (Fig. 7d), and the short horn-shaped CNTs accounted for about 25–30%. Even if the reaction time was extended to 24 h, the tube/particle ratio did not increase obviously, so the reaction time was selected as 10 h. If the products were not washed with salt acid, the horn-shaped CNTs still had one open end, and no obvious catalyst particle was observed on its top. If the products were not washed with distilled water or ethanol, the CNTs and CNSs could not yet be observed by SEM, so we think that the nanostructures could be wrapped with sodium. If the reagents were not added with sodium, pentachloropyridines could not be carbonized at 350 °C, so the sodium plays an important role in growth of the CNTs. On the basis of above experiments, a sodium-catalysis-reduction solid–liquid–solid (SLS) growth mechanism could be suggested via the root growth [22], similar to the CNT growth process by the reaction of CO_2 with Li [23]. Because the reaction temperature increases gradually, when approaching 150 °C, both pentachloropyridine (m.p. 124–6 °C) and sodium (m.p. 97.8 °C) were dissolved into liquid completely, and the reaction took place on the interface to form solid carbon spheres (Fig. 8a and b). When the reaction temperature reached 350 °C, fluidity of sodium liquids increased so that the sodium droplets were coated with CN_x and formed core-shell structure (nuclei). If the droplets were completely coated with CN_x, the core-shell structure would grow into hollow nanospheres as sodium core was consumed. When sodium droplets were partly coated with CN_x, connected with sodium liquid at the bottom, and formed the conical shape, it could control the growth of the nanotubes in the conical shape. As the carbon materials were sequentially fed at the bottom of CNTs, the nanotubes continuously grew towards the upper side (Fig. 8c), while nitrogen atoms were partly released. After the reaction closed, sodium particles at the bottom were washed with ethanol and water in order to form horn-shaped open end.

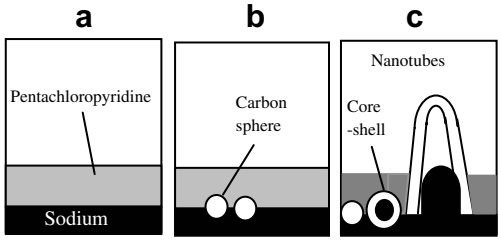

Fig. 8. Schematic diagram of the growth process. (a) coexistence of sodium and pentachloropyridine lquids (at ~130–150 °C); (b) solid carbon nanospheres (CNSs) were formed on the interfaces of above liquids (above 150 °C); (c) hollow or solid CNSs and the horn-shaped CNTs were formed (above 350 °C).

4. Conclusions

In summary, we provide a method preparing nitrogen-doped horn-shaped CNTs by the reduced reaction of pentachloropyridine with sodium, and reasonably explain the sodium-catalyzed growth mechanism of the CNTs. As the reaction temperature increases, the N/C ratio of the products decreases, and is lower than 0.2 (that of C_5N ring) (at 150–400 °C). Therefore it does not support the growth mechanism of C_5N six-number-ring self-assemblage. Under present condition, only when the reaction temperature reached 350 °C, the CNTs could form.

Acknowledgements

We acknowledge the financial support from Nanjing University Talent Development Foundation and the National Science Foundations of China (No. 20671050).

References

[1] Iijima S. Helical microtubules of graphitic carbon. Nature 1991; 354(6348):56–8.
[2] Tang ZK, Zhang LY, Wang N. Superconductivity in 4 Å single-walled carbon nanotubes. Science 2001;292(5526):2462–5.
[3] Tans SJ, Verschueren ARM, Dekker C. Room-temperature transistor based on a single carbon nanotube. Nature 1998;393(6680):49–52.
[4] Frank S, Poncharal P, Wang ZL. Carbon nanotube quantum resistors. Science 1998;280(5370):1744–6.
[5] Pradhan BK, Kyotani T, Tomita A. Nickel nanowires of 4 nm diameter in the cavity of carbon nanotubes. Chem Commun 1999; 14:1317–8.
[6] Ajayan PM. Nanotubes from carbon. Chem Rev 1999;99:1787–99.
[7] Li WZ, Wen JG, Sennett M, Ren ZF. Clean double-walled carbon nanotubes synthesized by CVD. Chem Phys Lett 2003;368(3–4): 299–306.
[8] Deepak FL, John NS, Govindaraj A, Kulkarni GU, Rao CNR. Nature and electronic properties of Y-junctions in CNTs and N-doped CNTs obtained by the pyrolysis of organometallic precursors. Chem Phys Lett 2005;411(4–6):468–73.
[9] Wu XC, Tao YR, Lu YN, Dong L, Hu Z. High-pressure pyrolysis of melamine route to nitrogen-doped conical hollow and bamboo-like carbon nanotubes. Diam Relat Mater 2006;15(1):164–70.
[10] Terrones M, Ajayan PM, Banhart F, Blase XD, Carroll L, Charlier JC, et al. N-doping and coalescence of carbon nanotubes: synthesis and electronic properties. Appl Phys A 2002;74(3):355–61.
[11] Suenaga K, Johansson MP, Hellgren N, Broitman E, Wallenberg LR, Colliex C, et al. Carbon nitride nanotubulite densely-packed and well-aligned tubular nanostructures. Chem Phys Lett 1999;300(5–6): 695–700.
[12] Stephan O, Ajayan PM, Colliex C, Redlich Ph, Lambert JM, Bernier P, et al. Doping graphitic and carbon nanotube structures with boron and nitrogen. Science 1994;266(5191):1683–4.
[13] Terrones M, Terrones H, Grobert N, Hsu WK, Zhu YQ, Hare JP, et al. Efficient route to large arrays of CN_x nanofibers by pyrolysis of ferrocence/melamine mixtures. Appl Phys Lett 1999;75(25):3932–4.
[14] Wu C, Guo Q, Yin P, Li T, Yang Q, Xie Y. Synthesis of nitrogen-doped carbon nanostructures by the reaction of small molecule

carbon halides with sodium azide. J Phys Chem B 2005; 109(7):2597–604.
[15] Jiang Y, Wu Y, Zhang S, Xu C, Yu W, Xie Y, et al. A catalytic-assembly solvothermal route to multiwall carbon nanotubes at a moderate temperature. J Am Chem Soc 2000;122(49):12383–4.
[16] Yan YH, Cui J, Chan-Park MB, Wang X, Wu Y. Systematic studies of covalent functionalization of carbon nanotubes via argon plasma-assisted UV grafting. Nanotechnology 2007;18:115712–8.
[17] Chen H, Yang Y, Hu Z, Huo KF, Ma YW, Chen Y, et al. Synergism of C_5N six-membered ring and vapor–liquid–solid growth of CN_x nanotubes with pyridine precursor. J Phys Chem B 2006;110:16422–7.
[18] Lou ZS, Chen QW, Wang W, Zhang YF. Synthesis of carbon nanotubes by reduction of carbon dioxide with metallic lithium. Carbon 2003;41:3063–74.
[19] Liang EJ, Ding P, Zhang HR, Guo XY, Du ZL. Synthesis and correlation study on the morphology and Raman spectra of CN_x nanotubes by thermal decomposition of ferrocene/ethylenediamine. Diam Relat Mater 2004;13(1):69–73.
[20] Sveningsson M, Morjan RE, Nerushev OA, Sato Y, Backstrom J, Campbell EEB, et al. Raman spectroscopy field-emission properties of CVD-grown carbon-nanotube films. Appl Phys A 2001;73(4): 409–18.
[21] Yang QH, Hou PX, Unno M, Yamauchi S, Saito R, Kyotani T. Dual Raman features of double coaxial carbon nanotubes with N-doped and B-doped multiwalls. Nano Lett 2005;5(12):2465–9.
[22] Suenaga K, Yudasaka M, Colliex C, Iijima S. Radially modulated nitrogen distribution in CN_x nanotubular structures prepared by CVD using Ni phathalocyanine. Chem Phys Lett 2000;316(5–6):365–72.
[23] Lou Z, Chen C, Chen Q. Growth of conical carbon nanotubes by chemical reduction of $MgCO_3$. J Phys Chem B 2005;109(21): 10557–60.